Polypodiopsida and Nanotechnology

Subjects: Nanoscience & Nanotechnology

Contributor: Irina Fierascu, Radu Claudiu Fierascu, Camelia Ungureanu, Oana Alexandra Draghiceanu, Liliana Cristina Soare

The species belonging to the *Polypodiopsida* class have been part of human culture since the beginning of civilization, often being utilized due to the presence of antimicrobial substances (such as alkaloids, terpenes as tannins, saponins, anthraquinones, cardiac glycosides, etc.). Application of the ferns in nanotechnology is presented with practical examples.

Keywords: Polypodiopsida ; nanotechnology ; nanomaterials

1. Introduction

The term “nano” is encountered in all aspects of our daily life, often being regarded as the ultimate “bottleneck” breaker in various technological areas [1][2][3]. Day by day, nanomaterials represent a more and more a common aspect of our lives, in as much as we are becoming accustomed to nanomaterials-based personal care products, pharmaceutical products or even agricultural products [4]. The “nano” approach can help to improve the solubility of poorly water-soluble active substances and increase their bioavailability [5], increase storage stability of active substances, and develop more efficient drug carriers, thus leading to next generation nanomedicine tools [6].

2. *Polypodiopsida* and the Nanomaterials

Although ferns are not as commonly encountered as other classes of plants in the nanotechnology area [7], the literature study revealed several important studies in this field, suggesting a potential field of application for this underutilized class, particularly in the nanomaterials phytosynthesis process. The phytosynthesis mechanism involves the reduction and stabilization of the metallic nanoparticles by the phytoconstituents of the vegetal material (**Figure 1**). As in the case of any phytosynthesis process, in the case of fern extracts, applications can be distinguished several factors influencing the morphology of the final nanoparticles (NPs) and thus their potential applications [7]:

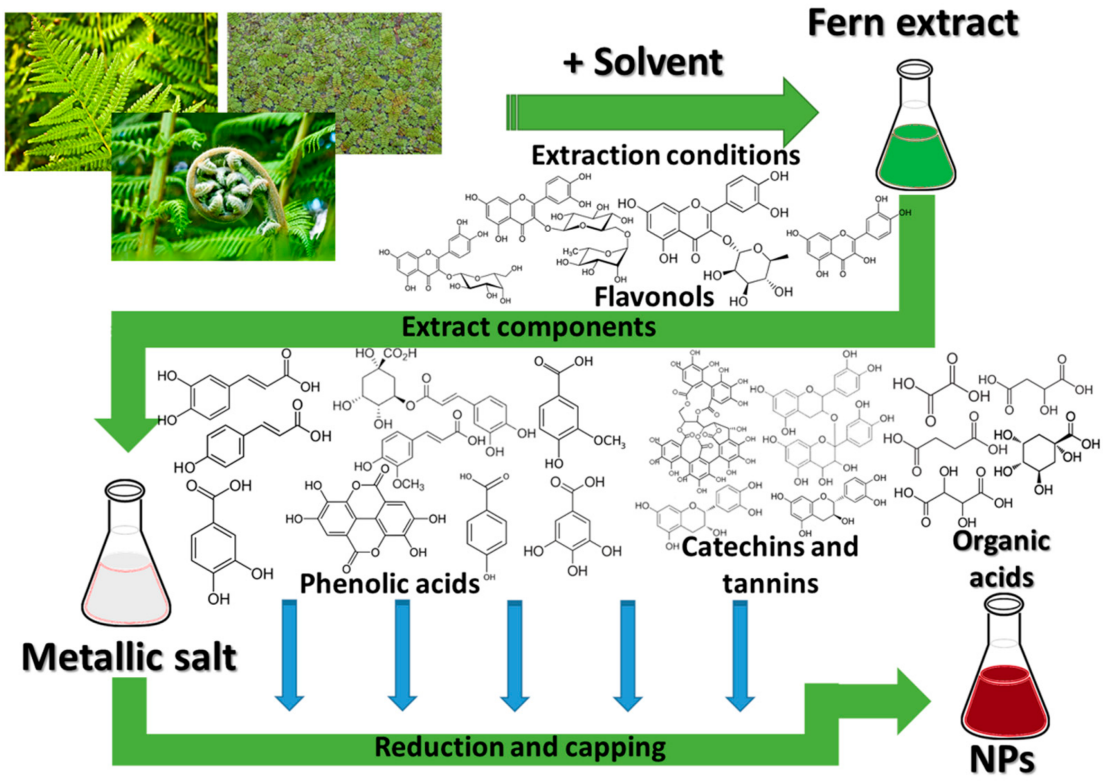

Figure 1. Phytosynthesis process and some of the involved phytoconstituents of ferns.

- factors related to the vegetal extract used: the intrinsic properties of the plants, related to their phytocomponents, the part of the plant used, extraction procedure, used solvents, the vegetal material to solvent ratio, plant pre-treatment, etc.;

- factors related to the phytosynthesis process: concentration of the metallic salt precursors, reaction conditions (temperature, pH, reaction time), extract to metallic salt ratio, etc.

As all these factors can affect the NPs' properties, studies should be considered for comparative evaluation of their influence. In the case of other plant classes, it is not surprising to identify studies on similar vegetal materials, with different results, as the authors used slightly different conditions; even the geographical region from which the vegetal material is collected can influence the NPs' characteristics, as the plants' composition can be influenced by the environmental factors [8].

The general process for the phytosynthesis of NPs using fern extracts, in which the main role for the reduction and capping of the metals is assigned to different phytoconstituents of the plants in the Polypodiopsida class, is depicted in **Figure 1**.

2.1. Nanoparticle *Phytosynthesis* Using Ferns

As the *terrestrial ferns* are the most encountered, their use for the nanoparticle phytosynthesis is also more frequent. Several authors present the phytosynthesis of different types of nanoparticles, most often silver or gold. Other types of NPs (copper oxide, iron) or composites are also encountered, although to a lesser extent. Among those nanoparticles, AgNPs are the most common subject of research, due to the well-known antimicrobial potential of silver, well-known from ancient times [9]. The differences between silver in the nanoparticle and in its ionic form, in terms of interaction with living cells, were recently discussed by other authors [9]. Elaborating the aspects detailed in the cited work, the use of silver in its nanoparticle form can be considered advantageous over the application of silver ions (even though some studies report inferior antibacterial properties for NPs, compared with silver ions [10]), due to several aspects:

- silver ions can bind to form different insoluble precipitates, which can negatively affect their properties [9];

- particularly for the case of phytosynthesized nanoparticles, the use of different phytocomponents as capping agents can not only contribute to an increase in their antimicrobial or antioxidant potential (for example) [7], but can decrease their toxic potential against non-target organisms [7], which is actually lower for NPs, compared with silver ions [11];

- the large surface area to volume ratio of nanoparticles (an element common for all types of NPs) provides better contact with microorganisms, thus increasing their antimicrobial potential, as well as contributing to their successful application in other areas [12].

2.2. Potential Applications of Phytosynthesized Nanoparticles

The phytosynthesis of the NPs leads to the attainment of nanoparticles with characteristics depending on the extract used. Being closely correlated with the natural extract, the phytosynthesized NPs finds applications in areas in which the extracts have a historical use, such as antioxidant or antimicrobial fields, in which various phytoconstituents (such as phenolic acids, flavonoids, terpenes, carotenoids and proanthocyanidins) have proven applicability.

The main area in which the fern-phytosynthesized NPs are expected to find application is represented by antimicrobial applications (and in this area are found most of the published studies on fern-mediated NPs). The antimicrobial mechanism of the phytosynthesized NPs is well established, being previously presented by the group [7], mainly involving the disruption of cellular membrane and on the generation of ROS (reactive oxygen species). Silver nanoparticles (a common subject of antimicrobial studies) represent the main subject regarding nanoparticles phytosynthesis using ferns. Multiple studies evaluated the antimicrobial potential of AgNPs obtained using fern extracts. Results (**Table 1**) presented either as inhibition zones or as MIC/MCBE (minimum inhibitory concentration/minimal concentration values for biofilm eradication) values are usually close to the positive control used for the experiments (a commercial antimicrobial). Significant results were obtained by Miljković et al. [13] using AgNPs obtained by *Equisetum arvense* L. especially against the Gram-negative bacteria, with an MIC of 0.72 mg/L.

Table 1. Potential applications of nanoparticles phytosynthesized using ferns [1].

Fern Used	Applied NPs	Application Results	Ref.
		Antimicrobial potential	
Asplenium scolopendrium L.	AgNPs, 10–12 nm	Evaluated against *Staphylococcus aureus*, *Pseudomonas aeruginosa*; MIC-1/32 (against *S. aureus*); MCBE-1/16 (*P. aeruginosa*);	[14]
Dryopteris crassirhizoma Nakai (1920)	AgNPs, spherical, 5–60 nm	Evaluated against *Bacillus cereus* and *P. aeruginosa*; best inhibition zones (IZ): 10 mm/250 µg under green LED (*B. cereus*); 6 mm/250 µg under green LED (*P. aeruginosa*).	[15]
Equisetum arvense L.	AgNPs, nearly spherical, 10–60 nm	Evaluated against *Escherichia coli*, *S. aureus*, *Candida albicans*, commercial probiotic *Saccharomyces boulardii*; Selective activity against *E. coli* (effective at low concentrations-0.72 mg/L);	[13]
Equisetum arvense L.	AgNPs, spherical, 170.5 nm	evaluated against *Salmonella enterica, B. cereus, Listeria monocytogenes, Enterococcus faecium, S. aureus, Aeromonas hydrophila*) IZ (mm) = 11.64/10.75/12.46/9.68/12.53/10.80	[16]
Equisetum giganteum L.	AgNPs, spherical, 20 nm	Evaluated against *E. coli, S. aureus, Alternaria alternata, Chaetomium globosum*; Fungal resistance test and antibacterial biofilm tests after incorporation in waterborne paints; active against all strains; MIC-3.3/13.3/3.3/67.5 µg/mL; paint films inhibited fungal and bacterial biofilm development	[17]
Dicranopteris linearis (Burm.f.) Underw	AgNPs, spherical, 40–60 nm	Evaluated against *Bacillus subtilis, Klebsiella pneumoniae* and *Salmonella typhi*; IZ (mm) = 21.01/20.1/19 at 75 ppm	[18]
Gleichenella pectinata (Willd.) Ching	AgNPs, spherical, 7.51 nm.	Evaluated against *P. aeruginosa, E. coli, K. pneumoniae* and *C. albicans*; IZ (mm) = 15/11/10/13 at 5 mM	[19]
Nephrolepis biserrata (Sw.) Schott	RuNPs, ~26 nm	Evaluated against *Aspergillus flavus*; 50% inhibition at 0.6 mL;	[20]
Nephrolepis cordifolia (L.) K. Presl	SiO_2@Au–Ag composites (200–246 nm SiO_2 decorated with 3-nm AuNPs/AgNPs)	Evaluated against *E. coli, S. aureus*; IZ (mm) = 21/14	[21]
Adiantum philippense L.	AuNPs—spherical, triangular, 33.9 nm in AuNPs–amoxicillin composites	Evaluated against *E. coli, S. aureus, Staphylococcus epidermis, B. subtilis, B. cereus*, MRSA1, MRSA2, MRSA3, MRSA4; in vivo treatment of systemic MRSA infection : IZ (mm) = 31/30/19/35/38/16/15/12/12 MIC/MBC (mg/L) = 2/4; ½; ½; 16/32; 8/16; 16/32; 16/32; 16/32; 32/32. Survival rate at day 7 post-inoculation 96%	[22]
Adiantum philippense L.	AgNPs, quasi-spherical, 10–60 nm	Evaluated against *B. subtilis*, *Listeria monocytogenes*, *S. aureus*, *E. coli*, *K. pneumoniae, Salmonella typhimurium*; MIC = 105.41/17.55/17.85/12.36/17.84/28.77	[23]
Pteris ripartite Sw.	AgNPs, different morphologies, 32 nm	Evaluated against *B. subtilis*, *B. cereus, Bacillus megaterium*, *E. coli*, *Proteus vulgaris*, *Serratia marcescens*, *S. typhi*, *K. pneumoniae*, *Vibrio cholerae*, *Shigella sonnei*, *Enterobacter aerogenes*, *P. aeruginosa, A. niger*, *Aspergillus flavus*, *Fusarium oxysporum*, *Penicillium chrysogenum*, *Rhizopus oryzae*; IZ (mm) = 8.33 (*B. cereus*) − 24.33 (*P. aeruginosa*) at 10 mg/mL; MIC (at 10 mg/mL, 24 h) = 0.29 (*P. aeruginosa*) − 1.40 (*E. coli*);	[24]
Adiantum capillus-veneris L.	AgNPs, spherical, 18.4 nm	Evaluated against *E. coli* and *S. aureus*; IZ (mm) = 30/19 applied as “thick nanoparticle suspension”	[25]
Adiantum capillus-veneris L.	AuNPs	Evaluated against *E. coli, P. aeruginosa, Salmonella enterica, S. aureus, B. subtilis, Trichophyton rubrum, Scedosporium apiospermum, Aspergillus fumigates, A. niger, A. flavus*; IZ (mm) = 16 (*A. fumigates, S. apiospermum, S. enterica*) − 21 (*E. coli*)	[26]
Pteris quadriaurita Retz.	AuNPs	Evaluated against *E. coli, P. aeruginosa, S. enterica, S. aureus, B. subtilis, T. rubrum, S. apiospermum, A. fumigates, A. niger, A. flavus*; IZ (mm) = 14 (*T. rubrum*) − 18 (*S. aureus*)	[26]
Marsilea quadrifolia L.	AgNPs, spherical, 9–42 nm	Evaluated against *E. coli*; MIC = 0.5 nM;	[27]

Fern Used	Applied NPs	Application Results	Ref.
Salvinia molesta D. Mitch.	AgNPs, spherical, 12.46 nm	Evaluated against *E. coli, S. aureus*; IZ (mm) = 21/16 (at 50 ppm); MIC = 10.5/13 mg/L Cell viability loss = 95.8/92.6% after 8 h. at MIC	[28]
Cibotium barometz (L.) J. Sm.	AgNPs, spherical, 5–40 nm;	Evaluated against *E. coli, S. aureus, S. enterica, P. aeruginosa*; IZ (mm, AgNPs) = 16/17.5/12.5/12.5 at 45 µg/disc;	[29]
		Antioxidant potential	
Asplenium scolopendrium L.	AgNPs, < 50 nm	DPPH inhibition 81.34%/80.93% (rhizomes/leaves mediated NPs)	[30]
Equisetum arvense L.	AgNPs, spherical, 170.5 nm	$IC_{0.50}$ (reducing power activity) = 641.24 µg/mL; IC_{50} (ABTS/DPPH/NOx) = 210.16/92.90/62.52 µg/mL;	[16]
Nephrolepis biserrata (Sw.) Schott	RuNPs, ~26 nm	IC_{50} (mg/mL, DPPH, ABTS, SORS, HSA assays) = 0.986/0.852/1.265/1.389	[20]
Pteris tripartite Sw.	AgNPs, different morphologies, 32 nm	DPPH, chelating activity, Phosphomolybdenum, ABTS, HPSA assays: 47.90 (mg/L)/61.51 ± 0.61 (mg EDTA/g)/41.94 ± 2.29 (mg AAE/g)/8592.70 ± 614.2 (µmol Trolox/g)/16.20 ± 3.86 (%);	[24]
Adiantum capillus-veneris L.	AuNPs	Inhibition: ~90% (DPPH)/~70% (SORS)/~85% (HPSA)/~82% (HSA);	[26]
Pteris quadriaurita Retz.	AuNPs	Inhibition: ~81% (DPPH)/~60% (SORS)/~77% (HPSA)/~75% (HSA);	[26]
Marsilea quadrifolia L.	AuNPs, spherical, 10–40 nm	IC_{50} (DPPH) = 50 mg/L;	[31]
Leptochilus pteropus (Blume) Fraser-Jenk	AgNPs	IC_{50} = 47.0 µg/mL (DPPH)/35.8 µg/mL (HPSA)	[32]
Cibotium barometz (L.) J. Sm.	AgNPs, spherical, 5–40 nm; AuNPs, spherical, 5–20 nm,	IC_{50} (DPPH) = 1.4/1.22 mg/mL (AuNPs/AgNPs)	[29]
		Cytotoxic potential	
Asplenium scolopendrium L.	AgNPs, < 50 nm	Rhizomes extract mediated NPs-progressive time-related mitoinhibitory effect; for both NPs—increased frequency and variability of chromosomal aberrations in the *Allium cepa* assay	[30]
Asplenium scolopendrium L.	AgNPs, 10–12 nm	Significantly higher frequency of the total aberrant cells compared with the negative control sample in the *Allium cepa* assay	[14]
Equisetum arvense L.	AgNPs, nearly spherical, 10–60 nm	MTT assay (MC3T3-E1): Cytotoxic threshold: >2.25/> 4.5 mg L^{-1}, lower for smaller NPs	[13]
Equisetum arvense L.	AgNPs spherical, 170.5 nm	Trypan blue exclusion test (HepG2): 20% viability (at 1 mg/mL)	[16]
Nephrolepis cordifolia (L.) K. Presl	SiO_2@Au–Ag composites (200–246 nm SiO_2 decorated with 3 nm AuNPs/AgNPs)	MTT assay (human keratinocyte cells): 95% cell viability at 500 µg/mL	[21]
Adiantum philippense L.	AuNPs-spherical, triangular, 33.9 nm.	MTT assay (L929): 81% viability (AuNPs), 79% viability (AuNPs–amoxicillin composites)	[22]
Adiantum sp.	AgNPs, AuNPs	MTT assay: Cytotoxicity against MCF-7 cells at different concentrations (2.5 to 100 µg/mL); non-cytotoxic to HEK293 cells	[33]
Marsilea quadrifolia L.	AgNPs, spherical, 9–42 nm	MTT assay: Cell death: 40.04% (MCF-7)/55.88% (HeLa), with NP sonication	[27]
Marsilea quadrifolia L.	AuNPs, spherical, 17–40 nm	MTT assay (3T3-L1): Cell viability = 71.23% (100 µM) − 84.02% (30µM); glucose uptake = 60.86%	[34]

Fern Used	Applied NPs	Application Results	Ref.
Marsilea quadrifolia L.	AuNPs, spherical, 10–40 nm	MTT assay: IC_{50} = 45.88/52.01 mg/L (PA-1/A549)	[31]
Cibotium barometz (L.) J. Sm.	AgNPs, spherical, 5–40 nm; AuNPs, spherical, 5–20 nm,	MTT assay (RAW264.7 and MCF-7): AuNPs—no cell death at 0.1–10 mg/L; AgNPs—cytotoxicity at ≥ 10 mg/L against RAW264.7	[29]
Alsophila nilgirensis (Holttum) R.M. Tryon	AgNPs, spherical, 45–74 nm	Hatched shrimps bioassay: LC_{50} = 869.4 µL/10 mL	[35]
		Larvicidal potential	
Pteridium aquilinum (L.) Kuhn	AgNPs spherical, 35–65 nm	Against *Anopheles stephensi* Liston, 1901 in laboratory conditions: LC_{50} of 7.48 ppm (larva I), 10.68 ppm (II), 13.77 ppm (III), 18.45 ppm (IV), and 31.51 ppm (pupae); Larvicidal assays in the field: complete removal of *An. stephensi* population after 72 h (at 10 × LC_{50} in water reservoir)	[36]
Dicranopteris linearis (Burm.f.) Underw	AgNPs spherical, 40–60 nm	Against *Aedes aegypti* (Linnaeus in Hasselquist, 1762); laboratory conditions: LC_{50} = 18.905 ppm (I)/ 20.929 ppm (II)/23.187 ppm (III)/26.312 ppm (IV)/29.328 ppm (pupae); LC_{90} = 32.140 ppm (I)/35.489 ppm (II)/39.696 ppm (III)/44.418 ppm (IV)/48.511 ppm (pupae) Field larvicidal activity (by application in water storage tanks), ovicidal assay, oviposition deterrent activity 100% reduction in A. aegypti larval populations at 10 × LC_{50} (after 72 h); No hatching observed at 25 ppm; ER = 94.29% at 30 ppm;	[18]
Adiantum raddianum C. Presl	AgNPs, 9.69–13.9 nm	Against mosquito larvae, in laboratory conditions (*A. stephensi, A. aegypti*, and *Culex quinquefasciatus* Say, 1823): LC_{50} = 10.33/11.23/12.19 mg/L Low toxicity against non-target organisms (*Diplonychus indicus* Venk. et Rao and *Gambusia affinis* (S. F. Baird and Girard, 1853)), LC_{50} = 517.86–35.98 mg/L	[37]
		Phytotoxic potential	
Asplenium scolopendrium L.	AgNPs, 10–12 nm	NPs led to the reduction of the phytotoxic effect of the extracts in Triticum test	[14]
Adiantum philippense L.	CuONPs, quasi-spherical, 1–20 nm	Effect on *Lens culinaris* Medik: 91.26% seed germination, SVI = 4168.43, RWC = 84.37% at 0.025 mg/mL (optimum dose); optimum dose showed highest activity of defense enzymes and total phenolics; higher concentrations of NPs retard all the parameters	[38]
Alsophila nilgirensis (Holttum) R.M. Tryon	AgNPs, spherical, 45–74 nm	Effect on *Vigna radiata* (L.) R. Wilczek and *Sorghum vulgare* (L.). Seeds: Germination reduction: 38.65/100% (*V. radiata* and *S. vulgare*) at 50 mg/L	[35]
		Antidiabetic potential	
Equisetum arvense L.	AgNPs, spherical, 170.5 nm	IC_{50} (alpha-glucosidase) = 1.73 µg/mL;	[16]
		Anti-inflammatory potential	
Pteris tripartite Sw.	AgNPs, different morphologies, 32 nm	Anti-inflammatory activity Wistar albino adult female rats using the carrageenan-induced paw oedema method = 56.36%, 24 h., 100 mg/kg b.w.	[24]
		Hepatoprotective potential	
Azolla filiculoides Lam.	AuNPs, spherical, 17–40 nm	Significant increase in cell viability compared to the acetaminophen group (hepatocytes damage); significant reduction in the levels of LDH and CAT (dose dependent); AuNPs significantly reduced the GOT and GPT levels (50/10%), significantly increased the levels of GSH-Px and SOD (60–70%), drastically reduced the formation of MDA (60%) and ROS generation	[39]
		Catalytic properties	

Fern Used	Applied NPs	Application Results	Ref.
Diplazium esculentum **(Retz.) Sw.**	**AgNPs, different morphologies, 10–45 nm**	**Degradation of MB and RhB dyes under solar light illumination: complete disappearance of the adsorption peaks after 8 min.**	[40]
Diplazium esculentum **(Retz.) Sw.**	**AgNPs—spherical, 10–25 nm; AuNPs-different morphologies, 35–75 nm**	**Degradation of MV 6B, RB, 4-nitro phenol: Ag-98.4/98/96.8%; Au-98.2/98.9/97.3%**	[41]
Nephrolepis cordifolia **(L.) K. Presl**	**Au–Ag@AgCl, average size 30 nm**	**Synthesis of quinoline derivatives via three component coupling/hydroarylation/dehydrogenation of arylaldehyde, aniline, and phenyl acetylene derivatives; 96% yield for the composite applied, reaction conditions 9h, at reflux**	[42]
Nephrolepis cordifolia **(L.) K. Presl**	**SiO_2@Au–Ag composites (200–246 nm SiO_2 decorated with 3 nm AuNPs/AgNPs)**	**Solvent-free amidation of carboxylic acid catalyst: 97% yield for the composite applied, reaction conditions—8 h, 100 °C**	[21]
		Other environmental applications	
Nephrolepis cordifolia **(L.) K. Presl**	**FeNPs, spherical, 40–70 nm, other types of iron oxides**	**Cr(VI) removal: 90.93%**	[43]

[1] where: 3T3-L1—adipocyte cell lines; A549—adenocarcinomic human alveolar basal epithelial cells line; AAE—ascorbic acid equivalents; ABTS—azinobis 3-ethylbenzothiazoline-6-sulfonate; b.w.—body weight; CAT—catalase; DPPH—2,2-diphenyl-1-picrylhydrazyl; EDTA—ethylenediaminetetraacetic acid; ER—effective repellence; GOT—glutamate oxalate transaminase; GPT—glutamate pyruvate transaminase; GSH-Px—glutathione peroxidase; HEK293—human embryonic kidney 293 cells; HeLa—human cervical cancer cell line; HepG2—human liver cancer cell line; HPSA—hydrogen peroxide scavenging activity; IC_{50}—concentration required to result in a 50% antioxidant activity; LC_{50}—LC_{50} lethal concentration that kills 50% of the exposed organisms; LDH—lactate dehydrogenase; HSA—OH^- scavenging activity; L929—normal subcutaneous areolar adipose tissue cellular lines; MB—methylene blue; MBC—minimum bactericidal concentration; MC3T3-E1—mouse pre-osteoblast cells; MCBE—minimal concentration values for biofilm eradication; MCF-7—breast cancer cell line; MDA—malondialdehyde; MI—mitotic index; MIC—minimum inhibitory concentration; MP—mitotic phases; MRSA—Methicillin-resistant *Staphylococcus aureus;* M.V. 6B—Methyl Violet 6B; NOx—nitric oxide; PA-1—human ovarian teratocarcinoma cell line; RAW264.7—macrophage, Abelson murine leukaemia virus transformed cells line; RB—Rose Bengal; RhB—rhodamine B; ROS—reactive oxygen species; RWC—relative water content; SOD—superoxide dismutase; SORS—Superoxide Radical Scavenging; SVI—Seedling Vigour Index.

2.3. Development of Biogenic Nanoparticles

Another nanotechnological-related potential application of the ferns is represented by the attainment of biogenic nanoparticles (especially silica). This application is related to the capacity of ferns to take up different metals or metalloids, followed by the processing of the vegetal material, in order to obtain the amorphous, semi- or highly crystalline nanoparticles. As such, the vegetal material can be considered a source of metalloids (in the case of silica). For example, Mattos et al. [44] obtained amorphous spherical SiO_2 nanoparticles (7 nm) using horsetail fern (*E. arvense*) stems, by acid leaching (2% sulfuric acid, acid:solid ratio 10:1, temperature 100 °C), filtration and washing to neutral pH, drying (103 °C), and finally calcination for 1h at 650 °C in an air atmosphere. The authors used the biogenic silica as a carrier of a neem bark extract cross-linked with polycarboxylic acids biocide [45].

The same group used a three-step procedure to obtain agglomerated, irregular sphere-like silica nanoparticles from the leaves and stems of the same fern: hydroalcoholic extraction (1:1 (v/v) H_2O: EtOH, solid:liquid ratio of 1:10, 24 h); hydrolysis of the pre-extracted biomass (diluted sulfuric acid or water, solid:liquid ratio 1:10, heated at different temperatures and times); calcination of the washed solid after the hydrolysis for 1 h. [46].

Hosseini Mohtasham and Gholizadeh [47] also used the horsetail (entire plant) to obtain semi-crystallin silica nanoparticles using a procedure involving acid leaching (4 M hydrochloric acid, acid:solid ratio 50:1, refluxed 2 h); the treated vegetal material was subsequently centrifuged and washed to neutral pH, dried (50 °C) and calcinated (air atmosphere, heating rate of 1 degree/min, 2 h at 500 °C). A final composite, consisting of $H_3PW_{12}O_{40}$ loaded on the ethylenediamine immobilized on an epibromohydrin-functionalized Fe3O4@SiO_2 support, was tested by the authors; magnetite deposited

on the silica support was applied by the authors for the one-pot synthesis of dihydropyrano [2,3-c] pyrazole derivatives with a 99% yield [47].

Adinarayana et al. [48] used the water horsetail extract microwaved–pyrolyzed at 200 °C (30 min., using household microwave oven) for the attainment of highly crystalline silica nanoparticles (average size 2.5 nm) applied for the fluorescence detection of Fe^{3+} ions in water. Another species of the *Equisetum* genus (*Equisetum myriochaetum* Schltdl. and Cham., 1830—Mexican giant horsetail) was also used to obtain silica nanoparticles. Dried stems and branches were acid-digested (concentrated HNO_3/H_2SO_4 = 4:1, solid:acid ratio = 1:40, 48 h.), washed to a pH of 5, lyophilized and calcinated (air atmosphere, 650 °C, 5 h, heating rate 10 °C/min) by Sola-Rabada et al. [49] to obtain amorphous, 5-nm biogenic silica, used for enzyme immobilization. Following the same recipe, Bogireddy et al. [50] obtained biogenic amorphous silica from the stems of the giant horsetail, functionalized it with APTES and grown PtNPs on the obtained substrate (using a chemical route). The composite was applied for the catalytic reduction of 4-nitrophenol to 4-aminophenol, obtaining a complete reduction in 90 s. at room temperature [50].

References

1. Song, X.; Liu, Z.; Sun, D.D. Nano gives the answer: Breaking the bottleneck of internal concentration polarization with a nanofiber composite forward osmosis membrane for a high water production rate. Adv. Mater. 2011, 23, 3256–3260.
2. Park, J.S.; Kyhm, J.; Kim, H.H.; Jeong, S.; Kang, J.H.; Lee, S.; Lee, K.T.; Park, K.; Barange, N.; Han, J.Y.; et al. Alternative patterning process for realization of large-area, full-color, active quantum dot display. Nano Lett. 2016, 16, 6946–6953.
3. Fuertes, G.; Soto, I.; Carrasco, R.; Vargas, M.; Sabattin, J.; Lagos, C. Intelligent packaging systems: Sensors and nanosensors to monitor food quality and safety. J. Sens. 2016, 2016, 4046061.
4. Contado, C. Nanomaterials in consumer products: A challenging analytical problem. Front. Chem. 2015, 3, 48.
5. Gupta, S.; Kesarla, R.; Omri, A. Formulation strategies to improve the bioavailability of poorly absorbed drugs with special emphasis on self-emulsifying systems. ISRN Pharm. 2013, 2013, 848043.
6. Kumar, R.; Lal, S. Synthesis of Organic Nanoparticles and their Applications in Drug Delivery and Food Nanotechnology: A Review. J. Nanomater. Mol. Nanotechnol. 2014, 3, 4.
7. Fierascu, I.; Fierascu, I.C.; Brazdis, R.I.; Baroi, A.M.; Fistos, T.; Fierascu, R.C. Phytosynthesized metallic nanoparticles-between nanomedicine and toxicology. A brief review of 2019′s findings. Materials 2020, 13, 574.
8. Fierascu, I.; Fierascu, I.C.; Dinu-Pirvu, C.E.; Fierascu, R.C.; Anuta, V.; Velescu, B.S.; Jinga, M.; Jinga, V. A short overview of recent developments on antimicrobial coatings based on phytosynthesized metal nanoparticles. Coatings 2019, 9, 787.
9. Kędziora, A.; Speruda, M.; Krzyżewska, E.; Rybka, J.; Łukowiak, A.; Bugla-Płoskońska, G. Similarities and differences between silver ions and silver in nanoforms as antibacterial agents. Int. J. Mol. Sci. 2018, 19, 444.
10. Li, W.R.; Sun, T.L.; Zhou, S.L.; Ma, Y.K.; Shi, Q.S.; Xie, X.B.; Huang, X.M. A comparative analysis of antibacterial activity, dynamics and effects of silver ions and silver nanoparticles against four bacterial strains. Int. Biodeterior. Biodegrad. 2017, 123, 304–310.
11. Velicogna, J.R.; Ritchie, E.E.; Scroggins, R.P.; Princz, J.I. A comparison of the effects of silver nanoparticles and silver nitrate on a suite of soil dwelling organisms in two field soils. Nanotoxicology 2016, 10, 1144–1151.
12. Rai, M.; Yadav, A.; Gade, A. Silver nanoparticles as a new generation of antimicrobials. Biotechnol. Adv. 2009, 27, 76–83.
13. Miljković, M.; Lazić, V.; Davidović, S.; Milivojević, A.; Papan, J.; Fernandes, M.M.; Lanceros-Mendez, S.; Ahrenkiel, S.P.; Nedeljković, J.M. Selective antimicrobial performance of biosynthesized silver nanoparticles by horsetail extract against E. coli. J. Inorg. Organomet. Polym. Mater. 2020, 30, 2598–2607.
14. Fierascu, R.C.; Fierascu, I.; Lungulescu, E.M.; Nicula, N.; Somoghi, R.; Diţu, L.M.; Ungureanu, C.; Sutan, A.N.; Drăghiceanu, O.A.; Paunescu, A.; et al. Phytosynthesis and radiation-assisted methods for obtaining metal nanoparticles. J. Mater. Sci. 2020, 55, 1915–1932.
15. Lee, J.H.; Lim, J.M.; Velmurugan, P.; Park, Y.J.; Park, Y.J.; Bang, K.S.; Oh, B.T. Photobiologic-mediated fabrication of silver nanoparticles with antibacterial activity. J. Photochem. Photobiol. B 2016, 162, 93–99.
16. Das, G.; Patra, J.K.; Shin, H.S. Biosynthesis, and potential effect of fern mediated biocompatible silver nanoparticles by cytotoxicity, antidiabetic, antioxidant and antibacterial, studies. Mater. Sci. Eng. C 2020, 114, 111011.

17. Barberia-Roque, L.; Gámez-Espinosa, E.; Viera, M.; Bellotti, N. Assessment of three plant extracts to obtain silver nanoparticles as alternative additives to control biodeterioration of coatings. Int. Biodeterior. Biodegrad. 2019, 141, 52–61.

18. Rajaganesh, R.; Murugan, K.; Panneerselvam, C.; Jayashanthini, S.; Aziz, A.T.; Roni, M.; Suresh, U.; Trivedi, S.; Rehman, H.; Higuchi, A.; et al. Fern-synthesized silver nanocrystals: Towards a new class of mosquito oviposition deterrents? Res. Vet. Sci. 2016, 109, 40–51.

19. Femi-Adepoju, A.G.; Dada, A.O.; Otun, K.O.; Adepoju, A.O.; Fatoba, O.P. Green synthesis of silver nanoparticles using terrestrial fern (Gleichenia Pectinata (Willd.) C. Presl.): Characterization and antimicrobial studies. Heliyon 2019, 5, e01543.

20. Gupta, P.K.; Ranganath, K.V.S.; Dubey, N.K.; Mishra, L. Green synthesis, characterization and biological activity of synthesized ruthenium nanoparticles using fishtail fern, sago palm, rosy periwinkle and holy basil. Curr. Sci. 2019, 117, 1308–1317.

21. Sapkota, K.; Chaudhary, P.; Han, S.S. Environmentally sustainable route to SiO2@Au-Ag nanocomposites for biomedical and catalytic applications. RSC Adv. 2018, 8, 31311–31321.

22. Kalita, S.; Kandimalla, R.; Sharma, K.K.; Kataki, A.C.; Deka, M.; Kotoky, J. Amoxicillin functionalized gold nanoparticles reverts MRSA resistance. Mater. Sci. Eng. C 2016, 61, 720–727.

23. Chatterjee, A.; Khatua, S.; Acharya, K.; Sarkar, J. A green approach for the synthesis of antimicrobial bio-surfactant silver nanoparticles by using a fern. Dig. J. Nanomater. Biostruct. 2019, 14, 479–490.

24. Baskaran, X.; Vigila, A.V.G.; Parimelazhagan, T.; Muralidhara-Rao, D.; Zhang, S. Biosynthesis, characterization, and evaluation of bioactivities of leaf extract-mediated biocompatible silver nanoparticles from an early tracheophyte, Pteris tripartita Sw. Int. J. Nanomed. 2016, 11, 5789–5805.

25. Omidi, S.; Sedaghat, S.; Tahvildari, K.; Derakhshi, P.; Motiee, F. Biosynthesis of silver nanoparticles with Adiantum capillus-veneris l leaf extract in the batch process and assessment of antibacterial activity. Green Chem. Lett. Rev. 2018, 11, 544–551.

26. Rautray, S.; Rajananthini, A.U. Therapeutic potential of green, synthesized gold nanoparticles. BioPharm. Int. 2020, 33, 30–38.

27. Maji, A.; Beg, M.; Mandal, A.K.; Das, S.; Jha, P.K.; Kumar, A.; Sarwar, S.; Hossain, M.; Chakrabarti, P. Spectroscopic interaction study of human serum albumin and human hemoglobin with Mersilea quadrifolia leaves extract mediated silver nanoparticles having antibacterial and anticancer activity. J. Mol. Struct. 2017, 1141, 584–592.

28. Verma, D.K.; Hasan, S.H.; Banik, R.M. Photo-catalyzed and phyto-mediated rapid green synthesis of silver nanoparticles using herbal extract of Salvinia molesta and its antimicrobial efficacy. J. Photochem. Photobiol. B 2016, 155, 51–59.

29. Wang, D.; Markus, J.; Wang, C.; Kim, Y.J.; Mathiyalagan, R.; Aceituno, V.C.; Ahn, S.; Yang, D.C. Green synthesis of gold and silver nanoparticles using aqueous extract of Cibotium barometz root. Artif. Cells Nanomed. Biotechnol. 2017, 45, 1548–1555.

30. Sutan, N.A.; Fierascu, I.; Fierascu, R.C.; Manolescu, D.S.; Soare, L.C. Comparative analytical characterization and in vitro citogenotoxic activity evaluation of Asplenium scolopendrium L. leaves and rhizome extracts prior to and after Ag nanoparticles phytosynthesis. Ind. Crops Prod. 2016, 83C, 379–386.

31. Balashanmugam, P.; Mosachristas, K.; Kowsalya, E. In vitro cytotoxicity and antioxidant evaluation of biogenic synthesized gold nanoparticles from Marsilea quadrifolia on lung and ovarian cancer cells. Int. J. Appl. Pharmaceut. 2018, 10, 153–158.

32. Chick, C.N.; Misawa-Suzuki, T.; Suzuki, Y.; Usuki, T. Preparation and antioxidant study of silver nanoparticles of Microsorum pteropus methanol extract. Bioorg. Med. Chem. Lett. 2020, 30, 127526.

33. Zamani, S.; Idrees, D.; Jha, B.; Jha, A.K. Green synthesis of metal nanoparticles from adiantum frond: Comparative analysis on cancer cell lines. Nanosci. Nanotechnol. Asia 2020, 10, 806–816.

34. Chowdhury, A.; Kunjiappan, S.; Bhattacharjee, C.; Somasundaram, B.; Panneerselvam, T. Biogenic synthesis of Marsilea quadrifolia gold nanoparticles: A study of improved glucose utilization efficiency on 3T3-L1 adipocytes. In Vitro Cell Dev. Biol. Anim. 2017, 53, 483–493.

35. Johnson, M.; Santhanam, A.; Thangaiah, S.; Narayanan, J. Green synthesis of silver nanoparticles using Cyathea nilgirensis Holttum and their cytotoxic and phytotoxic potentials. Part. Sci. Technol. 2018, 36, 578–582.

36. Panneerselvam, C.; Murugan, K.; Roni, M.; Aziz, A.T.; Suresh, U.; Rajaganesh, R.; Madhiyazhagan, P.; Subramaniam, J.; Dinesh, D.; Nicoletti, M.; et al. Fern-synthesized nanoparticles in the fight against malaria: LC/MS analysis of

Pteridium aquilinum leaf extract and biosynthesis of silver nanoparticles with high mosquitocidal and antiplasmodial activity. Parasitol. Res. 2016, 115, 997–1013.

37. Govindarajan, M.; AlQahtani, F.S.; AlShebly, M.M.; Benelli, G. One-pot and eco-friendly synthesis of silver nanocrystals using Adiantum raddianum: Toxicity against mosquito vectors of medical and veterinary importance. J. Appl. Biomed. 2017, 15, 87–95.
38. Sarkar, J.; Chakraborty, N.; Chatterjee, A.; Bhattacharjee, A.; Dasgupta, D.; Acharya, K. Green synthesized copper oxide nanoparticles ameliorate defence and antioxidant enzymes in Lens culinaris. Nanomaterials 2020, 10, 312.
39. Kunjiappan, S.; Bhattacharjee, C.; Chowdhury, R. In vitro antioxidant and hepatoprotective potential of Azolla microphylla phytochemically synthesized gold nanoparticles on acetaminophen—Induced hepatocyte damage in Cyprinus carpio L. In Vitro Cell Dev. Biol. Anim. 2015, 51, 630–643.
40. Paul, B.; Bhuyan, B.; Purkayastha, D.D.; Dhar, S.S. Green synthesis of silver nanoparticles using dried biomass of Diplazium esculentum (retz.) sw. and studies of their photocatalytic and anticoagulative activities. J. Mol. Liq. 2015, 212, 813–817.
41. Sinha, T.; Ahmaruzzaman, M. Indigenous north eastern India fern mediated fabrication of spherical silver and anisotropic gold nano structured materials and their efficacy for the abatement of perilous organic compounds from waste water-A green approach. RSC Adv. 2016, 6, 21076–21089.
42. Sapkota, K.; Han, S.S. A novel environmentally sustainable synthesis of nanocomposites and their application as an efficient and recyclable catalyst for quinoline synthesis. New J. Chem. 2017, 41, 5395–5402.
43. Yi, Y.; Tu, G.; Tsang, P.E.; Xiao, S.; Fang, Z. Green synthesis of iron-based nanoparticles from extracts of Nephrolepis auriculata and applications for Cr(VI) removal. Mater. Lett. 2019, 234, 388–391.
44. Mattos, B.D.; Rojas, O.J.; Magalhães, W.L.E. Biogenic SiO2 in colloidal dispersions via ball milling and ultrasonication. Powder Technol. 2016, 301, 58–64.
45. Mattos, B.D.; Rojas, O.J.; Magalhaes, W.L.E. Biogenic silica nanoparticles loaded with neem bark extract as green, slow-release biocide. J. Clean. Prod. 2017, 142, 4206–4213.
46. Mattos, B.D.; Gomes, G.R.; de Matos, M.; Ramos, L.P.; Magalhães, W.L.E. Consecutive production of hydroalcoholic extracts, carbohydrates derivatives and silica nanoparticles from Equisetum arvense. Waste Biomass Valor. 2018, 9, 1993–2002.
47. Hosseini Mohtasham, N.; Gholizadeh, M. Nano silica extracted from horsetail plant as a natural silica support for the synthesis of H3PW12O40 immobilized on aminated magnetic nanoparticles (Fe3O4@SiO2-EP-NH-HPA): A novel and efficient heterogeneous nanocatalyst for the green one-pot synthesis of pyrano pyrazole derivatives. Res. Chem. Intermed. 2020, 46, 3037–3066.
48. Adinarayana, T.V.S.; Mishra, A.; Singhal, I.; Reddy, D.V.R.K. Facile green synthesis of silicon nanoparticles from Equisetum arvense for fluorescence based detection of Fe(III) ions. Nanoscale Adv. 2020, 9, 4125–4132.
49. Sola-Rabada, A.; Sahare, P.; Hickman, G.J.; Vasquez, M.; Canham, L.T.; Perry, C.C.; Agarwal, V. Biogenic porous silica and silicon sourced from Mexican Giant Horsetail (Equisetum myriochaetum) and their application as supports for enzyme immobilization. Colloid Surf. B 2018, 166, 195–202.
50. Bogireddy, N.K.R.; Sahare, P.; Pal, U.; Méndez, S.F.O.; Gomez, L.M.; Agarwal, V. Platinum nanoparticle-assembled porous biogenic silica 3D hybrid structures with outstanding 4-Nitrophenol degradation performance. Chem. Eng. J. 2020, 388, 124237.
